IRAQI JOURNAL OF APPLIED PHYSICS
Vol. 22, No. 4, October-December 2026, pp. 617-622

Mays W. Skakir
Thuraya Y. Sabri*
Aidah A. Al-Doori
Maha M. Ibrahim
Sahar N. Rashid

Department of Physics,
College of Science,
University of Tikrit,
Tikrit, IRAQ
* Corresponding author email:
thurayayarb90@tu.edu.iq

Effect of Diode Laser Irradiation on Structural and Optical Properties of Spin-Coated Cobalt Oxide Thin Films

Cobalt oxide (Co_3O_4) films were successfully prepared using the spin-coating technique. The structural properties were confirmed through X-ray diffraction analysis. These thin films underwent irradiation using three types of diode lasers which emitted light in three distinct wavelength ranges; namely red, green, and blue. From the results of the UV-visible spectroscopy, it was found that there was significant improvement in the absorbance properties of the films, particularly in the wavelength range of 350-500 nm. The results showed that the film exposed to the red laser had the highest enhancement. It was noted that the optical conductivity was improved after irradiation, while the light dependent resistor (LDR) decreased after laser irradiation. The results showed that the spin-coated Co_3O_4 thin film can be modified through irradiation from a diode laser, making it a suitable candidate for use in optoelectronics.

Keywords: Cobalt oxide; Laser irradiation; Optical properties; Light Dependent Resistor
Received: 3 March 2026; Revised: 28 April 2026; Accepted: 5 May 2026; Published: 1 October 2026

1. Introduction

Thin films are significant because they enable the study of the physical properties and structure of the crystals of the material, as well as the characteristics of the transition of the electrons. Moreover, the rapid development of electronic device technology, along with the increasing demand for miniaturization, accuracy, and efficiency, has led to the advancement of high-quality, cost-effective thin film fabrication techniques tailored to specific application requirements [1]. This is due to the very small thickness of thin films and high surface area, which enables them to possess distinct physical characteristics that make it the dominant technology in many uses, such as in solar cells, transistors, detectors, pumps, valves, diodes, photovoltaic cells, and sensors [2]. Thin films are usually defined as materials deposited in more than one layer with control over the arrangement of atoms, molecules, or ions over a solid surface, with a thickness of less than one micrometer. This allows scientists to tailor material properties for specific applications to meet the demands of newer technologies [3].

Cobalt oxide has attracted significant attention in recent years due to its affordability, non-toxicity, ease of synthesis, and environmental friendliness. It is a p-type transition metal oxide semiconductor [4,5]. It primarily exists in two distinct oxidation states, such as CoO and Co_3O_4. Because cobalt has a strong affinity for oxygen, it easily forms oxides because, when heated in the presence of oxygen, CoO readily oxidizes to Co_3O_4 [6,7]. Sol-gel is one of several techniques used to prepare cobalt oxide thin films [8,9]. One notable aspect of sol-gel synthesis is how easily the sol before gelation can be used in thin-film formation using standard methods like spin coating and dipping. Technically speaking, spin coating is different from dip-coating techniques. This method uses centrifugal force and solvent evaporation to form thin films [10].

In this work, the optical and structural properties of cobalt oxide thin films prepared by spin coating and irradiated with different diode lasers were investigated.

2. Experimental Part

Cobalt oxide (Co_3O_4) thin films were deposited using cobalt nitrate hexahydrate, $Co(NO_3)_2.6H_2O$. 4.656 g of it was dissolved in 40 mL of water distilled to produce a 0.4 M solution. The solution was stirred at 70°C for one hour using a magnetic stirrer in order to ensure complete dissolution. The solution was deposited onto glass substrates, which had been previously cleaned, using a spin coater at 2000 rpm for 40 s in order to produce uniform films. Six layers were coated to create consistent films, which were then annealed at 450°C in order to form cobalt oxide films. The films that were developed were illuminated through three diode lasers namely red laser (650 nm, 200 mW), green laser (532 nm, 1000 mW), and blue laser (450 nm, 500 mW). In light of the initial results obtained, the red laser was chosen for illumination at three time intervals (10, 20, and 30 s). The optical properties were analyzed using UV–Visible spectrophotometry.

A light source and light dependent resistor (LDR) was also used to measure the photoconductivity of the prepared samples before and after laser irradiation, as shown in the circuit in Fig. (1). The resistance was measured under illumination conditions using LDR setup.

3. Results and Discussion

XRD analysis was carried out on the synthesized cobalt oxide films before and after laser irradiation, as shown in Fig. (2). From the diagram, it can be noted that the synthesized cobalt oxide thin films display a polycrystalline nature. Peaks corresponding to a cubic spinel structure for Co_3O_4 were obtained, which corroborates well with JCPDS card no. 42-1467. There was no evidence of any other phase formation after the laser treatment, hence signifying the stability of the phase composition. Well-defined peaks were observed at certain 2θ values of ~31.2°, 36.8°, 44.8°, 59.3°, and 65.2°. This proves the successful formation of phase pure Co_3O_4 without any secondary phases like CoO and other impurities [11,12]. Nevertheless, certain changes occurred in intensity, broadening, and shifting of the peak after the irradiation process, indicating that changes have taken place in the microstructure but not the crystalline structure [11]. Changes like these are brought about by thermal effects induced by lasers, resulting in defects in the crystal lattices [13]. The variation in peak broadening indicates changes in crystallite size, where laser irradiation may promote either grain growth or fragmentation depending on the energy delivered to the film. In addition, the increase in peak broadening is associated with an increase in microstrain and dislocation density, reflecting the formation of structural defects such as oxygen vacancies and lattice imperfections [11,13].

Fig. (1) Circuit used to measure light dependent resistor (LDR)

A comparative study on various laser irradiations reveals that there is moderate alteration in crystallite size and strain in case of red laser; thus, it causes controlled defect generation and good crystallinity. However, when compared to the red laser, green and blue lasers cause high microstrain and dislocation density, as shown in table (1). The reason behind this observation could be their high energy and strong surface interaction [13,14].

The results of the crystallite size (about 21 nm) show that the films are indeed nanocrystalline. The values obtained for microstrains (about 10^{-3}) and dislocation densities suggest that the films are moderately distorted in their crystal structures. The structural modifications are in line with the improved optical behavior, suggesting that the defect and lattice distortions caused by laser irradiation affect the optoelectronic behavior of Co_3O_4 thin films [11,15].

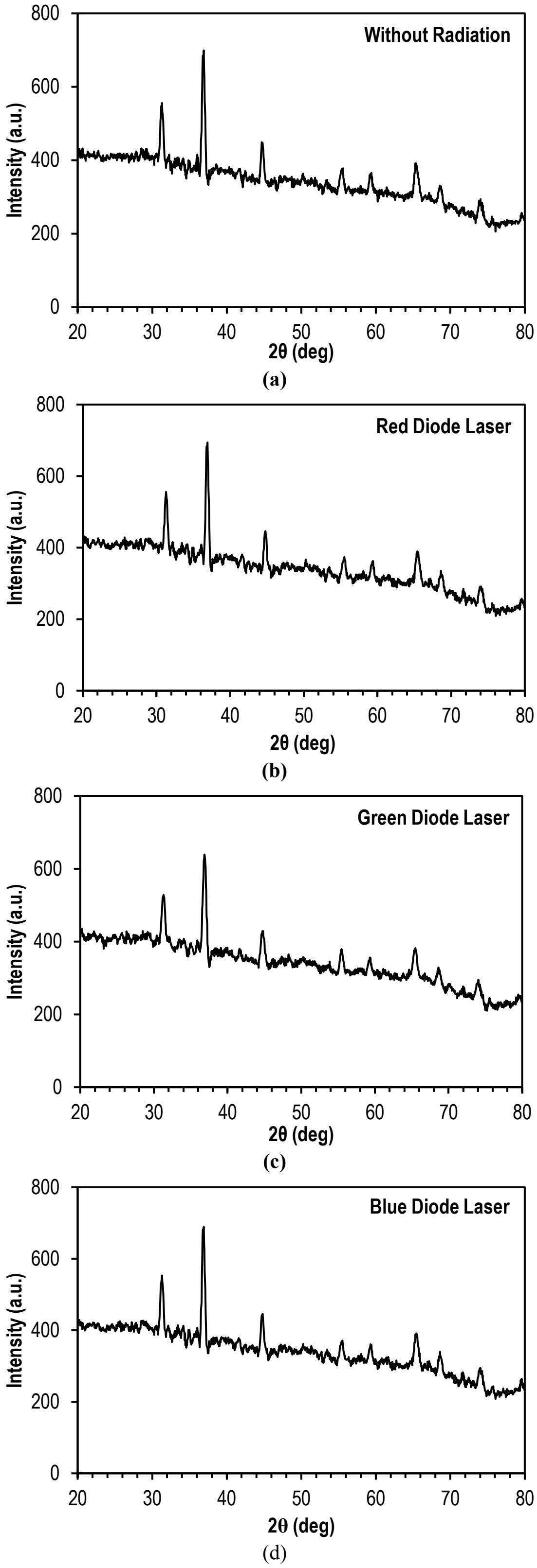

Fig. (2) XRD patterns of Co_3O_4 thin films (a) without irradiation, (b) red diode laser, (c) green diode laser, (d) blue diode laser

The microstructural parameters, such as microstrain (ε) and dislocation density (δ), have been evaluated using the XRD patterns to understand the defect structure of the synthesized Co_3O_4 thin films. The microstrain was evaluated using the formula $\varepsilon=\beta/(4\tan\theta)$, whereas the dislocation density was evaluated using the formula $\delta = 1/D^2$, where D denotes the value of the crystallite size obtained using the Debye-Scherrer's equation.

Optical characteristics of Co_3O_4 thin films prior to and post-laser irradiation have been investigated by means of UV-Visible spectrophotometry. From the study, notable changes in terms of absorbance, optical conductivity, bandgap, and LDR indicate that laser irradiation is capable of altering the electronic properties of the films. In Fig. (3), the absorbance spectra for Co_3O_4 thin films pre- and post-laser irradiation by a red (650 nm), green (532 nm), and blue (450 nm) laser diode are presented. However, there was found an appreciable rise in the absorbance after laser radiation in the UV-visible spectrum (approximately 350-500 nm).

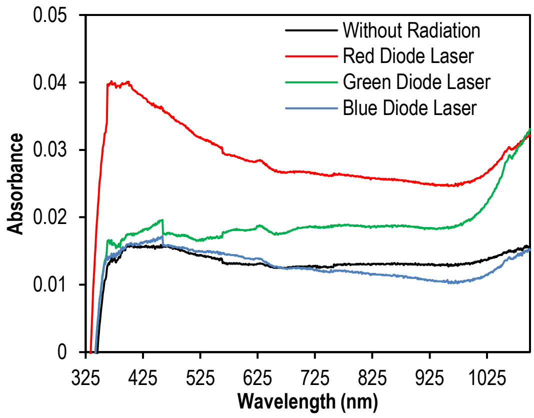

Fig. (3) Absorption spectra of Co_3O_4 thin films before and after irradiation with different types of lasers

It is essential to highlight that there was an unequal intensity of the utilized laser beams (Red beam: 200 mW, Green beam: 1000 mW, Blue beam: 500 mW). As such, the variance is affected by both factors - wavelength and intensity. Nevertheless, better results of the red laser can indicate more prominent influence of the penetration depth.

This increased absorption can be explained by laser-induced defects that are created in the material structure of Co_3O_4, namely oxygen vacancies and cobalt defects [13,16]. The energy states created within the band gap through defects result in better absorption and conduction of photons. The variation in laser performance can be explained based on the interaction depth. Shorter wavelengths (blue and green) have higher absorption coefficients, leading to surface-limited interaction and localized defect formation. In contrast, the red laser penetrates deeper into the film, resulting in a more uniform distribution of defects throughout the film thickness [17]. This uniform defect engineering improves charge carrier mobility and reduces recombination probability [14], thereby enhancing optical conductivity and overall absorbance.

Figure (4) presents the absorbance spectra under red laser irradiation for different exposure times (10, 20, and 30 s). The absorbance increases significantly at 10 s, particularly in the near-UV region (350-420 nm), followed by a slight decrease at longer irradiation times. This behavior indicates a competition between defect generation at short exposure times and defect saturation or partial structural relaxation at longer times [15,18].

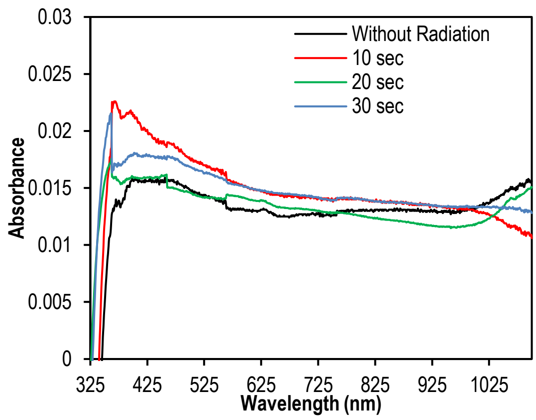

Fig. (4) Absorption spectra of Co_3O_4 thin films after irradiation with a red diode laser at different times

In case of optical conductivity spectroscopy (Figs. 5 and 6), an obvious increment has been observed post irradiation [19], mainly in the UV regime. The increase has been associated with higher number of carriers due to defect states, making the transitions more efficient.

From Fig. (7), there is a marginal difference in the values of the optical band gaps after irradiation, which have values of 1.60 eV, 1.66 eV, and 1.70 eV for red, green, and blue lasers, respectively. These values are consistent with reported direct band gap values of Co_3O_4. The increase in the optical band gap with laser irradiation can be explained by the reduction of defect-related states within the band gap, particularly oxygen vacancies, which leads to a shift in the absorption edge toward higher photon energies. Furthermore, localized thermal effects during laser exposure may enhance structural ordering and reduce disorder, resulting in improved electronic structure and a slight widening of the band gap [20].

For time-dependent irradiation (Fig. 8), the band gap slightly decreases at short exposure time (10 s), followed by stabilization at longer times. This behavior is associated with the initial formation of defect states, followed by saturation and partial relaxation effects.

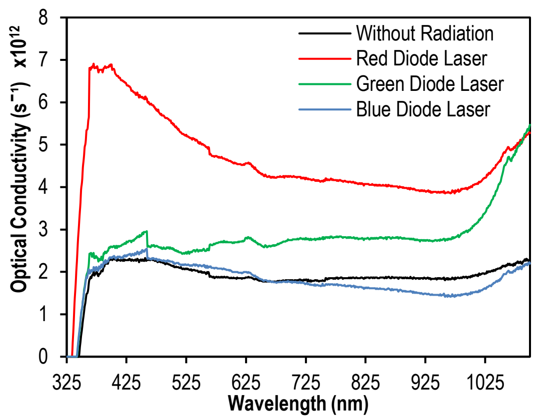

Fig. (5) Optical conductivity of Co_3O_4 thin films before and after irradiation with different types of lasers

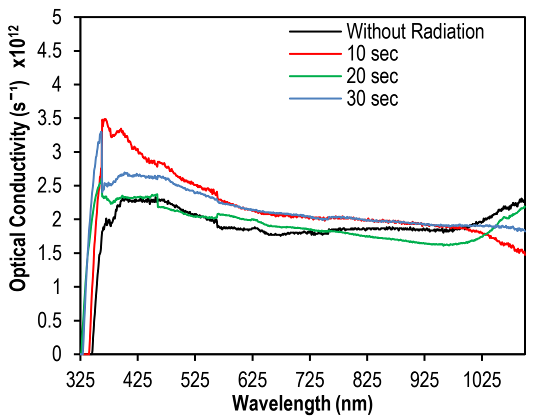

Fig. (6) Optical conductivity of Co_3O_4 thin films after irradiation with a red diode laser at different times

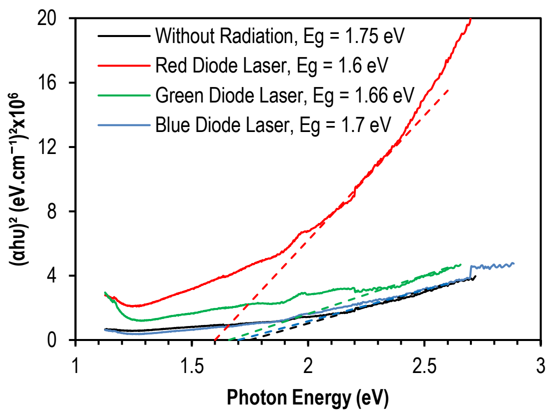

Fig. (7) Optical energy gap value for Co_3O_4 thin films before and after irradiation with different types of lasers

The effects on light dependent resistor (LDR) (Figs. 9 and 10) have clearly shown a drop following exposure to the laser beam, and the red laser showed the most minimal values. This suggests an increase in conductivity owing to enhanced carrier density and minimized recombination. The observed enhancement in absorbance, optical conductivity, and reduction in LDR can be explained by laser-induced defect engineering. The generation of controlled defects modifies the electronic structure and improves charge transport properties. These results demonstrate that diode laser irradiation is an effective and controllable technique for tuning the optoelectronic performance of Co_3O_4 thin films.

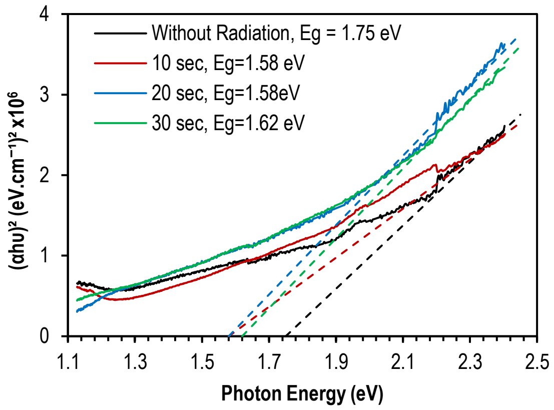

Fig. (8) Energy gap for Co_3O_4 thin films after irradiation with a red diode laser at different times

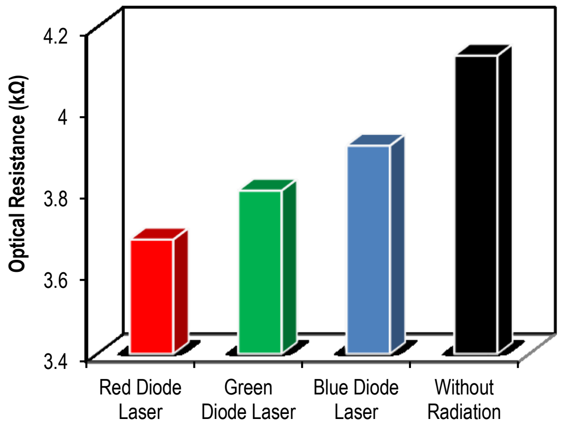

Fig. (9) LDR values for Co_3O_4 films before and after irradiation with different types of lasers

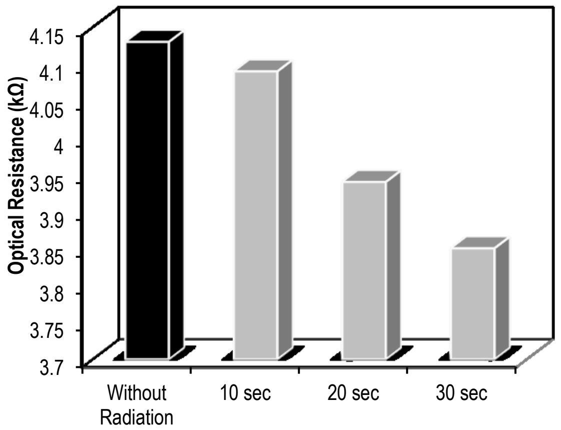

Fig. (10) LDR values for Co_3O_4 thin films after irradiation with a red diode laser at different times

4. Conclusion

Co_3O_4 thin films were successfully deposited through the spin-coating method, followed by modification using diode laser irradiation. The formation of a polycrystalline cubic spinel structure with nanoscale crystallite size was confirmed. Enhancement in the absorbance and optical conductivity was observed when the films were subjected to laser radiation. Variations in the optical band gap were found to be minimal, signifying the stability of the fundamental energy bands in the material, while the variations may be attributed to the modification of the bands due to defects in the material. It can be concluded that using a relatively inexpensive method of laser irradiation, as a post-processing method, can greatly enhance the optoelectronic properties of transition metal oxide films.

References

[1] S. Rubin et al., "The world of advanced thin films: Design, fabrication, and applications", *Fusion Multidiscip. Res.*, 4 (2023) 393-406.

[2] A.P. Arun et al., "Thin Films for Next Generation Technologies: A Comprehensive Review of Fundamentals, Growth, Deposition Strategies, Applications, and Emerging Frontiers", *Processes*, 13(12) (2025) 3846.

[3] J. Oke and T.C. Jen, "Atomic layer deposition and other thin film deposition techniques: From principles to film properties", *J. Mater. Res. Technol*., 21 (2022) 2481-2514.

[4] N. Kouidri, S. Rahmane and A. Allag, "Substrate temperature-dependent properties of sprayed cobalt oxide thin films", *J. Mater. Sci: Electron*., 30(2) (2019) 1153–1160.

[5] N.A.H. Hashim and F.J. Kadhim, "Structural and Optical Characteristics of Co_3O_4 Nanostructures Prepared by DC Reactive Magnetron Sputtering", *Iraqi J. Appl. Phys.*, 18(4) (2022) 31-36.

[6] L. Lukashuk et al., "Operando insights into CO oxidation on cobalt oxide catalysts by NAP-XPS, FTIR, and XRD", *ACS Catal*., 8(9) (2018) 8630–8641.

[7] N.A.H. Hashim, F.J. Kadhim and Z.S. Abdulsattar, "Characterization of Electrochromism and Photoelectrochromism of N-Doped TiO_2 and Co_3O_4 Thin Films Prepared by DC Reactive Magnetron Sputtering: Comparative Study", *Iraqi J. Appl. Phys.*, 19(1) (2023) 5-12.

[8] S.A. Al Kiey, A.A. Sery and H.K. Farag, "Sol-gel synthesis of nanostructured cobalt oxide in four different ionic liquids", *J. Sol-Gel Sci. Technol.,* 106 (2023) 37-43.

[9] Y.A. Wicaksono et al., "Synthesis and characterisation of cobalt oxide (Co_3O_4) using sol-gel auto combustion method with stirring time variations", *AIP Conf. Proc*., 2489 (2022) 030031.

[10] Y. Yunus et al., "Review of the Common Deposition Methods of Thin-Film Pentacene, Its Derivatives, and Their Performance", *Polymers*, 14(6) (2022) 1112.

[11] M. Abdel-Rafea, A. Eid and N.M. Mustapha, "The effect of annealing on the structure, morphology, and optical properties of Co_3O_4 thin films prepared using a modified dip coating technique", *Mater. Sci. Eng. B*, 290 (2023) 116294.

[12] H. Ghannam, I. Oumouna and A. Chahboun, "Influence of deposition time on the structural, optical, and electrochemical properties of sprayed Co_3O_4 thin films:, *Next Mater.,* 10 (2026) 101364.

[13] S. Huang et al., "Recent advances in irradiation-mediated synthesis and tailoring of inorganic nanomaterials for photo-/electrocatalysis", *Nanoscale Adv*., 7 (2025) 384-418.

[14] H. Kim, J. Lee and S. Yoon, "Laser-induced defect engineering and optical property modulation in transition metal oxide thin films", *Appl. Surf. Sci*., 615 (2023) 156345.

[15] M.A. Abdel-Rahman, S.H. Mohamed and A.M. Salem, "Effect of laser irradiation on structural and optical properties of Co_3O_4 thin films", *J. Mater. Sci. Electron.,* 34 (2023) 1423.

[16] A.A.C. Silva et al., "Tuning the photoconductivity of Co_3O_4 thin films by defect engineering", *Appl. Surf. Sci.,* 606 (2022) 154943.

[17] Z.B. Ali, N. Bakr and M. Kareem, "Synthesis and Characterization of (Co_3O_4-CuO) Thin Films with Varying Mixture Ratios", *Passer J.,* 7(1) (2025) 70-79.

[18] P. Priyadarshini et al., "Time-dependent laser irradiation-induced kinetics of changes in linear–nonlinear optical properties of $Bi_{15}In_{20}Se_{65}$ thin films for IR applications", *J. Appl. Phys*., 133(6) (2023) 063104.

[19] S.K. Vijitha, K. Mohanraj and R.P. Jebin, "Structural, Optical, and Surface modifications by varying precursor concentrations on Spray Deposition of In doped Co_3O_4 thin films for Electro chemical application", *Chem. Phys. Impact*, 6. (2023) 100143.

[20] M. Batzill and U. Diebold, "The surface and materials science of tin oxide", *Prog. Surf. Sci.*, 79(2-4) (2005) 47-154.

Table (1) XRD parameters of the prepared Co_3O_4 thin films

Sample	2θ (deg.)	FWHM (deg.)	d_{hkl} (Å)	D (nm)	(hkl)	Microstrain (ε)	Dislocation Density (nm^{-2})
Without Radiation	31.222	0.3936	2.86482	21.0	(220)	6.17×10^{-3}	2.27×10^{-3}
	36.8242	0.4428	2.44084	18.9	(311)	5.80×10^{-3}	2.80×10^{-3}
	44.7204	0.246	2.0265	34.9	(400)	2.61×10^{-3}	8.21×10^{-4}
	55.5412	0.5412	1.65461	16.6	(422)	5.75×10^{-3}	3.63×10^{-3}
	59.4081	0.3936	1.55581	23.2	(511)	3.90×10^{-3}	1.86×10^{-3}
	65.3144	0.3936	1.42869	24.0	(440)	3.60×10^{-3}	1.74×10^{-3}
	68.6607	0.492	1.367	19.6	(531)	4.10×10^{-3}	2.60×10^{-3}
	73.9212	0.6888	1.28219	14.4	(620)	5.10×10^{-3}	4.82×10^{-3}
Red Diode Laser	31.2241	0.4428	2.86463	18.6	(220)	5.70×10^{-3}	2.89×10^{-3}
	36.8215	0.4428	2.44101	18.9	(311)	5.80×10^{-3}	2.80×10^{-3}
	44.7151	0.3936	2.02673	21.8	(400)	4.90×10^{-3}	2.10×10^{-3}
	55.5279	0.492	1.65497	18.2	(422)	5.50×10^{-3}	3.01×10^{-3}
	59.3128	0.3936	1.55809	23.2	(511)	3.90×10^{-3}	1.86×10^{-3}
	65.4323	0.4428	1.4264	21.3	(440)	4.70×10^{-3}	2.20×10^{-3}
	68.7142	0.492	1.36606	19.6	(531)	4.10×10^{-3}	2.60×10^{-3}
	73.9109	0.6888	1.28234	14.4	(620)	5.10×10^{-3}	4.82×10^{-3}
Green Diode Laser	31.3957	0.4428	2.84937	18.6	(220)	5.70×10^{-3}	2.89×10^{-3}
	36.8908	0.4428	2.43658	18.9	(311)	5.80×10^{-3}	2.80×10^{-3}
	44.9138	0.4428	2.01822	19.4	(400)	5.20×10^{-3}	2.65×10^{-3}
	55.4544	0.492	1.657	18.2	(422)	5.50×10^{-3}	3.01×10^{-3}
	59.2969	0.492	1.55847	18.6	(511)	5.70×10^{-3}	2.89×10^{-3}
	65.5396	0.492	1.42432	19.2	(440)	5.30×10^{-3}	2.71×10^{-3}
	68.6937	0.5904	1.36642	16.3	(531)	6.20×10^{-3}	3.76×10^{-3}
	73.9428	0.5904	1.28187	16.8	(620)	6.00×10^{-3}	3.54×10^{-3}
Blue Diode Laser	31.2304	0.3936	2.86407	21.0	(220)	6.17×10^{-3}	2.27×10^{-3}
	36.8217	0.4428	2.441	18.9	(311)	5.80×10^{-3}	2.80×10^{-3}
	44.7182	0.3936	2.02659	21.8	(400)	4.90×10^{-3}	2.10×10^{-3}
	55.5159	0.4428	1.6553	20.3	(422)	5.30×10^{-3}	2.43×10^{-3}
	59.3249	0.4428	1.5578	20.6	(511)	5.20×10^{-3}	2.35×10^{-3}
	65.51	0.5412	1.4249	17.5	(440)	6.00×10^{-3}	3.26×10^{-3}
	68.5814	0.492	1.36838	19.5	(531)	4.20×10^{-3}	2.63×10^{-3}
	73.9162	0.6888	1.28227	14.4	(620)	5.10×10^{-3}	4.82×10^{-3}

